Applied Physics Letters ARTICLE scitation.org/journal/apl

Effects of proton irradiation-induced point defects on Shockley–Read–Hall recombination lifetimes in homoepitaxial GaN *p–n* junctions

Cite as: Appl. Phys. Lett. **122**, 113505 (2023); doi: 10.1063/5.0141781
Submitted: 9 January 2023 · Accepted: 1 March 2023 ·
Published Online: 14 March 2023

Tetsuo Narita,[1,a)] Masakazu Kanechika,[2] Kazuyoshi Tomita,[2] Yoshitaka Nagasato,[3] Takeshi Kondo,[2] Tsutomu Uesugi,[2] Satoshi Ikeda,[3] Masayoshi Kosaki,[4] Tohru Oka,[4] and Jun Suda[2,5]

AFFILIATIONS

[1]Toyota Central R&D Labs., Inc., Nagakute 480-1192, Japan
[2]Institute of Materials and Systems for Sustainability (IMaSS), Nagoya University, Nagoya 464-8601, Japan
[3]MIRISE Technologies Corporation, Toyota 470-0309, Japan
[4]Toyoda Gosei Co., Ltd., Ama, Aichi 490-1207, Japan
[5]Department of Electronics, Graduate School of Engineering, Nagoya University, Nagoya 464-8603, Japan

[a)]**Author to whom correspondence should be addressed:** tetsuo-narita@mosk.tytlabs.co.jp

ABSTRACT

This work examined the intentional generation of recombination centers in GaN *p–n* junctions on freestanding GaN substrates. Irradiation with a 4.2 MeV proton beam was used to create a uniform distribution of vacancies and interstitials across GaN p^+/n^- and p^-/n^+ junctions through anode electrodes. With increasing proton dose, the effective doping concentrations were found to be reduced. Because the reduction in the doping concentration was much higher than the hydrogen atom concentration, this decrease could not be attributed solely to carrier compensation resulting from interstitial hydrogen atoms. In fact, more than half of the electron and hole compensation was caused by the presence of point defects. These defects evidently served as Shockley–Read–Hall (SRH) recombination centers such that the SRH lifetimes were reduced to several picoseconds from several hundred picoseconds prior to irradiation. The compensation for holes in the p^-/n^+ junctions was almost double that for electrons in the p^+/n^- junctions. Furthermore, the SRH lifetimes associated with p^-/n^+ junctions were shorter than those for p^+/n^- junctions for a given proton dose. These differences can be explained by variations in the charge state and/or the formation energy of intrinsic point defects in the *p*-type and *n*-type GaN layers. The results of the present work indicate the asymmetry of defect formation in GaN based on the fact that intrinsic point defects in *p*-type GaN readily compensate for holes.

An understanding of the properties of point defects is an important aspect of the engineering of *p–n* junctions in semiconductor devices. The point defects appearing in silicon (Si) have been well characterized and, in fact, can be intentionally created via irradiation to control the switching performance of power devices.[1,2] These defects act as carrier recombination centers, and so, the carrier lifetime can be optimized by tuning the irradiation conditions. In the case of silicon carbide (SiC) incorporated into power devices having ultrahigh blocking voltages, it has been reported that carrier lifetimes are sometimes limited by the quality of the epitaxially grown SiC layer,[3,4] and they are also affected by the device fabrication process.[5,6] Based on a study involving the intentional creation of recombination centers via electron irradiation, Danno *et al.*[7] established that $Z_{1/2}$ centers in 4H-SiC greatly limit increases in the lifetime of carriers and inhibit the effective conductivity modulation in bipolar devices. Thus, particle irradiation is a useful approach to the quantitative evaluation of recombination dynamics because this technique allows defect concentrations to be controlled.

Gallium nitride (GaN) is also a potential component of power devices operating at relatively high frequencies, at which faster switching rates are expected. Carrier recombination in GaN has, therefore, also been studied using bulk crystals,[8–10] epitaxially grown layers,[9–11] and GaN layers processed by ion implantation.[12] Early research involving *n*-type GaN layers and crystals used samples with high threading dislocation densities (greater than $10^8\,\mathrm{cm}^{-2}$), for which photoluminescence lifetimes were limited to several hundred picoseconds,[8] for which threading dislocations greatly affect nonradiative recombination.[13] However, recent improvements in growth technologies have increased

the carrier lifetime to the nanosecond scale, which is quite significant with regard to direct transitions in this material.[8] These improvements have allowed quantitative analyses of the relationship between carrier lifetime and point defects. Kojima *et al.*[11] determined that the minority carrier lifetime in *n*-type GaN with a low dislocation density on the order of $10^6\,cm^{-2}$ was reduced upon increasing the carbon concentration in the material. It is important to evaluate the intrinsic point defects appearing in GaN, similar to prior assessments of $Z_{1/2}$ centers in SiC, because these defects can be introduced during device fabrication processes, such as ion implantation, dry etching, oxide or metal deposition, and annealing.

In the present study, point defects were intentionally introduced into homoepitaxial GaN *p*–*n* junctions having dislocation densities on the order of $10^6\,cm^{-2}$ using proton irradiation with varying doses. Although the appearance of proton-induced deep levels near both band edges has been previously investigated,[14,15] there have been few studies on midgap recombination centers in GaN specimens processed via particle irradiation. In the work reported herein, the carrier lifetimes were determined by analyzing Shockley–Read–Hall (SRH) recombination current plots having slopes with an ideality factor of 2.[16] This approach provides an advantage in that recombination dynamics near the *p*–*n* junction can be examined such that the resulting data can be directly connected to device performance. Although this approach has been applied to the analysis of epitaxially grown GaN *p*–*n* junctions,[17,18] *p*–*n* junctions in which defect concentrations have been intentionally modified have not yet been studied. Carrier recombination typically occurs on the side of the *p*–*n* junction where there is a lower level of doping. In addition, the stability of point defects and the charge state can differ between conduction types as well as the Fermi level. This work also examined the effect of the conduction type using GaN specimens having p^+/n^- and p^-/n^+ junctions. The results clearly demonstrate that intrinsic point defects in *p*-type GaN readily compensate for holes and, thus, reduce the recombination lifetime.

GaN *p*–*n* junctions were grown by metalorganic vapor phase epitaxy on freestanding GaN substrates having threading dislocation densities on the order of $10^6\,cm^{-2}$. Going from bottom to top, the layered structure was composed of a 0.2 μm thick n^{++}-type buffer layer doped with Si at a density of $2\times10^{18}\,cm^{-3}$, a 3 μm thick *n*-type GaN layer, a 2.5 μm thick *p*-type GaN layer, and a 0.1 μm thick p^{++}-type contact layer. By varying the doping concentrations in the *n*-type and *p*-type layers, both p^+/n^- and p^-/n^+ junctions were produced. The Mg and Si concentrations in the p^+/n^- junction referred to herein as w32 were 3.5×10^{17} and $4.5\times10^{16}\,cm^{-3}$, respectively, while those in the p^-/n^+ junction referred to as w34 were 6.5×10^{16} and $2.1\times10^{17}\,cm^{-3}$, based on analyses by secondary ion mass spectrometry (SIMS). Each diode had a junction diameter of 340 μm and was isolated by a 3.6 μm deep sloped mesa penetrating through the *p*-type layer into the *n*-type layer. This structure was created using a photoresist reflow technique and a subsequent dry etching process.[19,20] A 220 μm diameter Ni/Au anode was subsequently formed on the top of the specimen, and a Ti/Al/Ni cathode electrode was applied to the back, as shown in Fig. 1(a).

After dividing the wafer into chips using a dicing method, the samples were irradiated with 4.2 MeV protons (H^+) at varying doses at the facilities of the SHI-ATEX Co., Ltd. A 137 μm thick aluminum (Al) absorber was inserted in the irradiation setup such that the H^+ profile peaked near the *p*–*n* junctions as shown in Fig. 1. The proton doses applied during these trials were 1×10^{12}, 3×10^{12}, 1×10^{13}, and $3\times10^{13}\,cm^{-2}$. SIMS analyses were used to establish the implantation depth profile for a 6 μm thick *n*-type GaN specimen doped with Si at a density of $2\times10^{16}\,cm^{-3}$ after exposure to a proton dose of $1\times10^{13}\,cm^{-2}$. An implantation simulation result was also supplied by SHI-ATEX Co., Ltd. and is presented in Fig. 1(b). The experimental H atom concentration was found to be approximately $1.2\times10^{16}\,cm^{-3}$ at the depth of the *p*–*n* junction, which was roughly half the value produced by the simulation. Furthermore, the H atom profile obtained from SIMS analysis was broader than that for the simulation. These discrepancies occurred because the simulation neglected scattering and absorption by the Al absorber. However, the relative intensity trends obtained from the simulation were meaningful. Based on the simulation, the concentrations of Ga vacancies (V_{Ga}) in the irradiated specimen were approximately ten times higher than the H concentrations. In addition, the present implantation conditions evidently created twice as many V_{Ga} as nitrogen vacancies (V_N). This can be

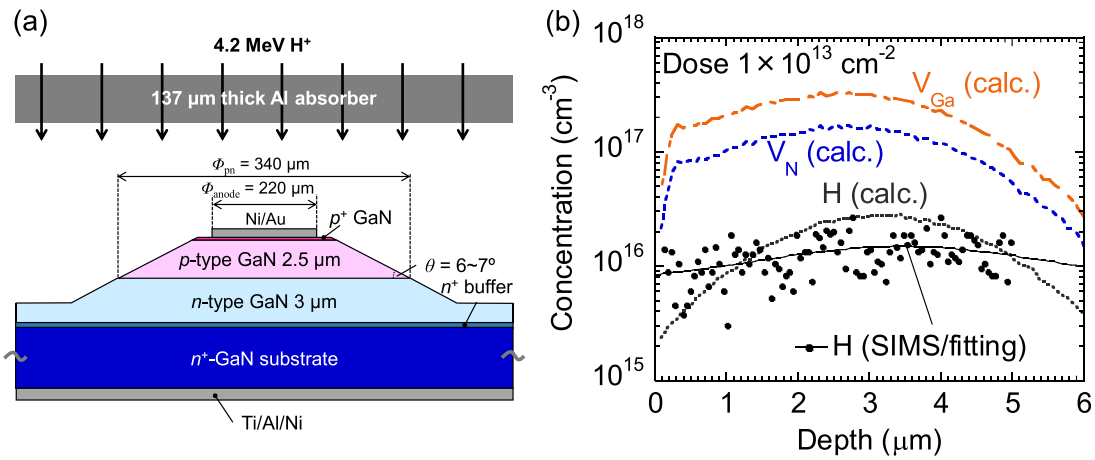

FIG. 1. (a) Diagram showing the experimental setup for proton irradiation of a GaN *p*–*n* diode structure. (b) H depth profile determined by SIMS (dots) and the simulated H, V_{Ga}, and V_N profiles (dashed lines) for a proton dose of $1\times10^{13}\,cm^{-2}$.

explained by that a Ga atom has a larger number of protons compared to an N atom, resulting in the larger collision cross section for implanted particles. Positron annihilation spectroscopy (PAS) was also used to assess the reference *n*-type specimen, and the data indicated that the vacancies in this sample comprised V_{Ga} and $V_{Ga}V_N$ types and were present at comparable levels. This result corresponded to the V_{Ga} to V_N ratio expected from the simulation. These PAS results will be discussed in detail in a future publication.

Figure 2(a) shows forward current density–voltage (*J*–*V*) curves obtained for the p^+/n^- junctions. In the case of the as-grown junction, an ideal slope of 2 was obtained for bias values below 2.5 V. The current component in this range was due to the SRH recombination current, J_{SRH}, defined as[18]

$$J_{SRH} \approx \frac{\pi n_i kT}{2\tau_{SRH} F_0} \exp\left(\frac{eV}{2kT}\right), \quad (1)$$

where n_i is the intrinsic carrier density, k is the Boltzmann constant, T is the measurement temperature, τ_{SRH} is the SRH recombination lifetime, F_0 is the electric field at the recombination depth [which can be estimated from capacitance–voltage (*C*–*V*) data], and e is the elementary charge. As such, the intercept of a semilog plot of the J_{SRH} values will give τ_{SRH}. Prior to irradiation, the extracted τ_{SRH} was 360 ps, although the τ_{SRH} value also varied over the range of 290–690 ps throughout the epitaxial wafer. The variation of the τ_{SRH} values might be caused by the in-plane distribution of carbon incorporation in the range of $(3–7)\times10^{15}$ cm^{-3}.[11] After proton irradiation at a dose of 1×10^{12} cm^{-2}, τ_{SRH} was reduced to 24 ps. Overall, increasing the proton dose decreased τ_{SRH}. After irradiation with a dose of 1×10^{13} cm^{-2}, τ_{SRH} was further decreased to 4.2 ps, and the series resistance above 2.7 V was greatly increased. The irradiation at a dose of 3×10^{13} cm^{-2} resulted in high resistivity. Ga vacancy complexes in GaN are known to act as effective SRH recombination centers due to the relatively large capture cross sections for these complexes,[10,21] and, based on the PAS results, the GaN specimens after proton irradiation contained V_{Ga} and $V_{Ga}V_N$. Previous photoluminescence studies suggest that $V_{Ga}V_N$ function as effective nonradiative recombination centers.[10,21] Even so, the impact of isolated V_{Ga} on SRH recombination is unclear because these vacancies are unlikely to form in as-grown GaN specimens.[22] The net doping concentration, N', was also estimated from *C*–*V* data, where N' is defined as $N_dN_a/(N_d + N_a)$, with N_d and N_a being the effective donor and the acceptor concentrations in the *n*-type and the *p*-type layers, respectively. From the data in Fig. 2(b), N' before irradiation was estimated to be 3.76×10^{16} cm^{-3}. It is evident from Table I that the net doping concentration decreased with increasing dose, and the *p*–*n* junction was fully depleted after irradiation with a dose of 3×10^{13} cm^{-2}.

In the case of the p^-/n^+ junction (w34), the τ_{SRH} values for the as-grown junction were in the range of 320–590 ps, as shown in Fig. 3(a). This range is comparable to that for the p^+/n^- junction as provided in Table I. Furthermore, the τ_{SRH} values were approximately one order of magnitude higher than those found for p^-/n^+ junctions in our previous study.[18] This improvement is probably attributed to the elimination of residual impurities, such as iron atoms, by controlling the growth conditions.[23] Iron atoms in GaN are known to act as effective SRH recombination centers.[24,25] The concentration of these species was suppressed to below the detection limit of the SIMS measurement (10^{14} cm^{-3}) in the present work. As a result, the τ_{SRH} values for the *p*-type layer exceeded the highest value of approximately 100 ps reported on the basis of a time-resolved photoluminescence examination of homoepitaxial *p*-type GaN specimens by Chichibu *et al.*[26]

After irradiation, reductions in both τ_{SRH} and the net doping concentration were also observed for the p^-/n^+ junctions (w34) although the data were quantitatively different from those obtained for p^+/n^- junctions (w32). For a proton dose of 3×10^{12} cm^{-2}, the τ_{SRH} value was decreased to 2.8 ps, which was much shorter than the value of 7.8 ps obtained for the p^+/n^- junction. Furthermore, the p^-/n^+ junction (w34) exhibited high resistivity after exposure to a H^+ dose greater than 1×10^{13} cm^{-2}, for which full depletion is observed in the *C*–*V* data in Fig. 3(b). That is,

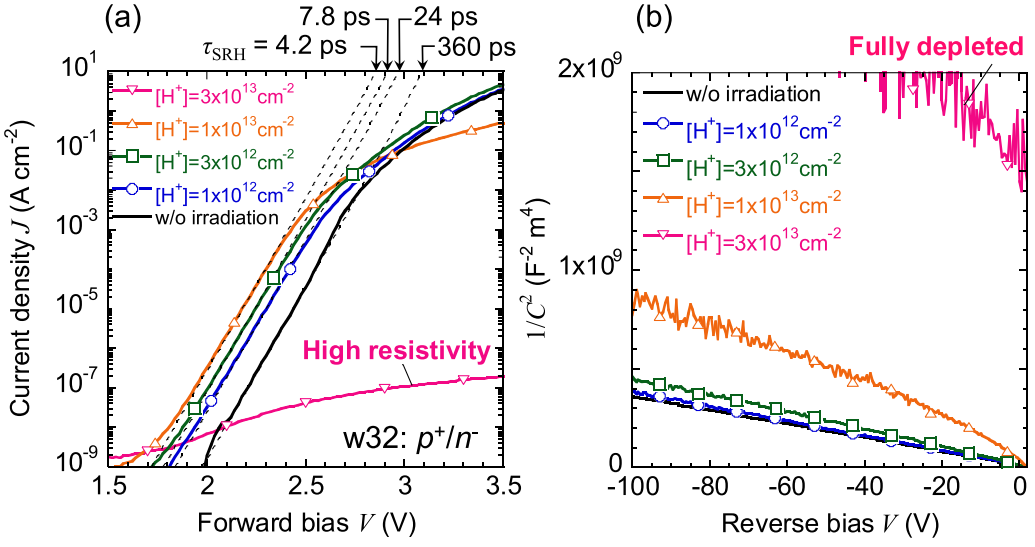

FIG. 2. (a) Forward *J*–*V* curves for p^+/n^- junctions (w32) irradiated at proton doses of 0 (w/o), 1×10^{12}, 3×10^{12}, 1×10^{13}, and 3×10^{13} cm^{-2}. The dashed lines indicate the components of the SRH recombination current for τ_{SRH} of 360, 24, 7.8, and 4.2 ps. (b) $1/C^2$–*V* plots for p^+/n^- junctions irradiated at the same proton doses as in (a).

TABLE I. Summary of doping densities, N', and SRH lifetimes before and after proton irradiation for p^+/n^- (w32) and p^-/n^+ (w34) junctions. N' values were estimated from *C–V* data. Three *p–n* diodes in the divided chip were examined at each proton dose.

	w32: $p^+(3.5\times10^{17}\ \mathrm{cm^{-3}})/n^-(4.5\times10^{16}\ \mathrm{cm^{-3}})$		w34: $p^-(6.5\times10^{16}\ \mathrm{cm^{-3}})/n^+(2.1\times10^{17}\ \mathrm{cm^{-3}})$	
Proton dose $\times10^{12}\ \mathrm{cm^{-2}}$	Doping density N' $\times10^{16}\ \mathrm{cm^{-3}}$	SRH lifetime ps	Doping density N' $\times10^{16}\ \mathrm{cm^{-3}}$	SRH lifetime ps
0	3.75–3.80	290–690	4.82–4.85	320–590
1	3.50	24–25	4.23–4.31	9.4–11
3	2.83–2.86	7.8–8.3	2.43–2.75	2.7–2.8
10	1.02–1.08	4.0–4.3	High resistivity	N/A
30	High resistivity	N/A	High resistivity	N/A

high resistivity in the p^-/n^+ junction is lower than that for the p^+/n^- junction. To eliminate the effects of the in-plane distribution of doping, the difference in the net doping concentration (ΔN) before and after irradiation was determined for each of the same devices, and Fig. 4(a) plots ΔN as a function of the H^+ dose for the p^+/n^- and p^-/n^+ junctions. Note that ΔN at a proton dose of $1\times10^{13}\ \mathrm{cm^{-2}}$ was $2.4\times10^{16}\ \mathrm{cm^{-3}}$ and so corresponded to twice the H concentration of $1.2\times10^{16}\ \mathrm{cm^{-3}}$ obtained from the SIMS analysis. First principles calculations have established that a single interstitial hydrogen atom (H_i) in GaN can compensate for one electron or one hole in an *n*-type or *p*-type layer.[27] Therefore, one half of the electron compensation effect observed for the p^+/n^- junction could be explained by the effect of H_i while the remaining half can be attributed to point defects. The degree of reduction in the net doping for the p^-/n^+ junction was 1.5–2 times higher than that for the p^+/n^-. This difference cannot be explained by the carrier compensation effect of H_i, and is, therefore, attributed to point defects. There are two possible reasons for the difference between the junctions. One is a variation in the charge state of point defects between the *n*-type and *p*-type layers. Here, we can assume that proton irradiation creates a number of $V_{Ga}V_N$ and the corresponding interstitials (Ga_i and N_i). In the case of an *n*-type layer, $V_{Ga}V_N$, Ga_i, and N_i will theoretically have charges of 2–, 1+, and 1–, respectively, resulting in a total charge of 2–.[28] However, in the case of a *p*-type layer, the charges are 3+ ($V_{Ga}V_N$), 3+ (Ga_i), and 2+ or 3+ (N_i), giving a total charge of 8+ or 9+.[28,29] Assuming only a pair comprising V_{Ga} and Ga_i, the total charges will be 2– and 2+ for *n*-type and *p*-type layers, respectively. Because some of the vacancies that were created in the present specimens were the $V_{Ga}V_N$ type, the effect of the charge state will be significant.

However, the charge state effect cannot explain the greater reduction in τ_{SRH} for the p^-/n^+ junction than for the p^+/n^- junction, as shown in Fig. 4(b). The other possible factor is related to variations in the stability of intrinsic point defects between *n*-type and *p*-type GaN. The Ga_i and N_i formation energies in *p*-type GaN are much lower than those in *n*-type GaN.[29] Frenkel defect pairs of vacancies and interstitials can partly recombine during irradiation because interstitials are mobile at a temperature near RT.[30] Indeed, ΔN was found to be much smaller than the vacancy concentration expected from the

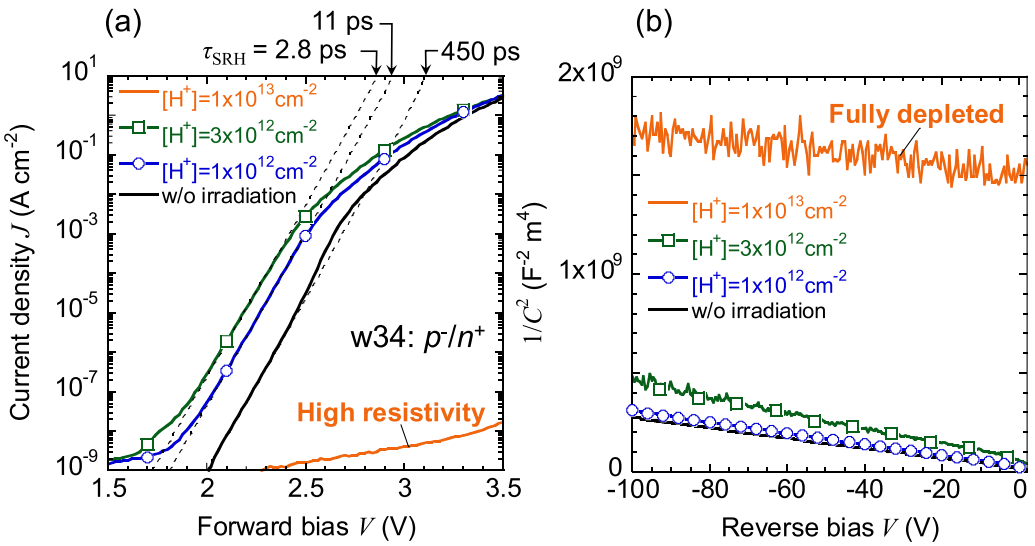

FIG. 3. (a) Forward *J–V* curves for p^-/n^+ junctions (w34) irradiated at proton doses of 0 (w/o), 1×10^{12}, 3×10^{12}, and $1\times10^{13}\ \mathrm{cm^{-2}}$. The dashed lines indicate the components of the SRH recombination current for τ_{SRH} of 450, 11, and 2.8 ps. (b) $1/C^2$–*V* plots for p^+/n^- junctions irradiated at the same proton doses as in (a). The data for a proton dose of $3\times10^{13}\ \mathrm{cm^{-2}}$ are not included here because no current flow was observed, and the p^--type layer was completely depleted.

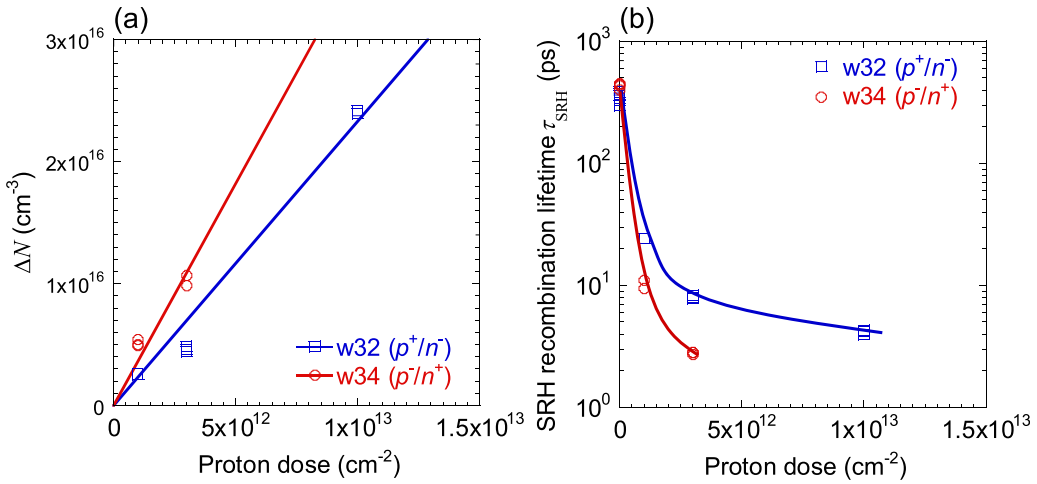

FIG. 4. (a) Change in effective doping density, ΔN, and (b) τ_{SRH} as functions of proton dose for p^+/n^- (w32) and p^-/n^+ (w34) junctions.

simulation, indicating partial annihilation. The extent of annihilation will, in turn, depend on the stability of interstitials. Due to the higher stability of Ga_i and N_i in *p*-type GaN, annihilation likely did not take place, resulting in a higher defect concentration. The annealing examination at a somewhat higher temperature than RT might be helpful for discussing such defect stabilities in both the conduction types of GaN. The temperature-dependence of SRH recombination lifetimes will be studied after carefully separating it from the annealing effect in the future.

In summary, this work demonstrated tuning of the SRH lifetime in GaN *p*–*n* junctions using proton irradiation. V_{Ga}-related defects created by irradiation are thought to have acted as recombination centers, and at least half of the carrier compensation was related to the presence of irradiation-induced point defects. More carriers were compensated for by point defects in *p*-type GaN, and the SRH lifetimes for p^-/n^+ junctions were shorter than those for p^+/n^- junctions. This difference was attributed to variations in the charge state and/or formation energies of point defects at different Fermi levels. The present results clearly indicate that holes in *p*-type GaN are readily compensated for by point defects and have shorter SRH lifetimes than electrons in *n*-type layers. This difference appears to originate from doping asymmetry. It should also be noted that *p*-type ion implantation requires a higher annealing temperature than *n*-type implantation.[31] This agrees with the finding that point defects in *p*-type GaN can trap more free carriers. As such, the removal of point defects is a crucial aspect of *p*-type activation. The results of the present study are expected to assist in future with regard to the fabrication of GaN power devices incorporating *p*–*n* junctions.

The authors thank Mr. Takahide Yagi and Mr. Joji Ito of SHI-ATEX Co., Ltd., for performing proton irradiation and irradiation simulations. The authors thank Dr. Akira Uedono of Tsukuba Materials Research Co., Ltd., who is also a professor at the University of Tsukuba, for assisting in the assessment of vacancy types using positron annihilation spectroscopy. The authors thank the Center for Integrated Research of Future Electronics, Transformative Electronics Facilities (C-TEFs) at Nagoya University for fabricating the devices used in this work.

AUTHOR DECLARATIONS

Conflict of Interest

The authors have no conflicts to disclose.

Author Contributions

Tetsuo Narita: Conceptualization (lead); Data curation (lead); Formal analysis (lead); Investigation (equal); Methodology (lead); Validation (equal); Visualization (lead); Writing – original draft (lead); Writing – review & editing (equal). **Jun Suda:** Conceptualization (equal); Formal analysis (equal); Funding acquisition (lead); Project administration (lead); Resources (equal); Supervision (lead); Validation (equal); Writing – review & editing (equal). **Masakazu Kanechika:** Conceptualization (equal); Data curation (equal); Formal analysis (equal); Investigation (equal); Resources (equal); Validation (equal); Writing – review & editing (supporting). **Kazuyoshi Tomita:** Conceptualization (equal); Data curation (equal); Formal analysis (supporting); Investigation (equal); Resources (equal); Validation (equal); Writing – review & editing (equal). **Yoshitaka Nagasato:** Data curation (equal); Formal analysis (supporting); Investigation (equal); Project administration (equal); Writing – review & editing (supporting). **Takeshi Kondo:** Data curation (supporting); Investigation (equal); Methodology (equal); Writing – review & editing (supporting). **Tsutomu Uesugi:** Data curation (supporting); Investigation (equal); Methodology (equal); Writing – review & editing (supporting). **Satoshi Ikeda:** Data curation (equal); Investigation (equal); Methodology (equal); Writing – review & editing (supporting). **Masayoshi Kosaki:** Data curation (supporting); Investigation (equal); Writing – review & editing (supporting). **Tohru Oka:** Data curation (supporting); Investigation (equal); Project administration (equal); Writing – review & editing (supporting).

DATA AVAILABILITY

The data that support the findings of this study are available from the corresponding author upon reasonable request.

REFERENCES

[1]B. J. Baliga and E. Sun, IEEE Trans. Electron Devices **ED-24**, 685 (1977).
[2]A. Mogro-Campero, R. P. Love, M. F. Chang, and R. F. Dyer, IEEE Electron Device Lett. **6**, 224 (1985).
[3]J. P. Bergman, O. Kordina, and E. Janzén, Phys. Status Solidi A **162**, 65 (1997).
[4]K. Danno, K. Hashimoto, H. Saitoh, T. Kimoto, and H. Matsunami, Jpn. J. Appl. Phys., Part II **43**, L969 (2004).
[5]T. Kimoto, Y. Nanen, T. Hayashi, and J. Suda, Appl. Phys. Express **3**, 121201 (2010).
[6]T. Hayashi, K. Asano, J. Suda, and T. Kimoto, J. Appl. Phys. **109**, 014505 (2011).
[7]K. Danno, D. Nakamura, and T. Kimoto, Appl. Phys. Lett. **90**, 202109 (2007).
[8]K. Kojima, Y. Tsukada, E. Furukawa, M. Saito, Y. Mikawa, S. Kubo, H. Ikeda, K. Fujito, A. Uedono, and S. F. Chichibu, Appl. Phys. Express **8**, 095501 (2015).
[9]S. F. Chichibu, A. Uedono, T. Onuma, T. Sota, B. A. Haskell, S. P. DenBaars, J. S. Speck, and S. Nakamura, Appl. Phys. Lett. **86**, 021914 (2005).
[10]S. F. Chichibu, A. Uedono, K. Kojima, H. Ikeda, K. Fujito, S. Takashima, M. Edo, K. Ueno, and S. Ishibashi, J. Appl. Phys. **123**, 161413 (2018).
[11]K. Kojima, F. Horikiri, Y. Narita, T. Yoshida, H. Fujikura, and S. F. Chichibu, Appl. Phys. Express **13**, 012004 (2020).
[12]K. Shima, H. Iguchi, T. Narita, K. Kataoka, K. Kojima, A. Uedono, and S. F. Chichibu, Appl. Phys. Lett. **113**, 191901 (2018).
[13]A. Pinos, S. Marcinkevičius, M. Usman, and A. Hallén, Appl. Phys. Lett. **95**, 112108 (2009).
[14]Z. Zhang, A. R. Arehart, E. Cinkilic, J. Chen, E. X. Zhang, D. M. Fleetwood, R. D. Schrimpf, B. McSkimming, J. S. Speck, and S. A. Ringel, Appl. Phys. Lett. **103**, 042102 (2013).
[15]Z. Zhang, A. R. Arehart, E. C. H. Kyle, J. Chen, E. X. Zhang, D. M. Fleetwood, R. D. Schrimpf, J. S. Speck, and S. A. Ringel, Appl. Phys. Lett. **106**, 022104 (2015).
[16]T. Kimoto, N. Miyamoto, and H. Matsunami, IEEE Trans. Electron Devices **46**, 471 (1999).
[17]Z. Hu, K. Nomoto, B. Song, M. Zhu, M. Qi, M. Pan, X. Gao, V. Prostasenko, D. Jena, and H. G. Xing, Appl. Phys. Lett. **107**, 243501 (2015).
[18]T. Maeda, T. Narita, H. Ueda, M. Kanechika, T. Uesugi, T. Kachi, T. Kimoto, M. Horita, and J. Suda, Jpn. J. Appl. Phys., Part 1 **58**, SCCB14 (2019).
[19]T. Maeda, T. Narita, H. Ueda, M. Kanechika, T. Uesugi, T. Kachi, T. Kimoto, M. Horita, and J. Suda, in *IEEE International Electron Devices Meeting* (IEEE, San Francisco, 2018), p. 687.
[20]T. Narita, Y. Nagasato, M. Kanechika, T. Kondo, T. Uesugi, K. Tomita, S. Ikeda, S. Yamaguchi, Y. Kimoto, M. Kosaki, T. Oka, J. Kojima, and J. Suda, Appl. Phys. Lett. **118**, 253501 (2021).
[21]S. F. Chichibu, K. Kojima, A. Uedono, and Y. Sato, Adv. Mater. **29**, 1603644 (2017).
[22]A. Alkauskas, C. E. Dreyer, J. L. Lyons, and C. G. Van de Walle, Phys. Rev. B **93**, 201304(R) (2016).
[23]T. Narita, M. Horita, K. Tomita, T. Kachi, and J. Suda, Jpn. J. Appl. Phys., Part 1 **59**, 105505 (2020).
[24]D. Wickramaratne, J. X. Shen, C. E. Dreyer, M. Engel, M. Marsman, G. Kresse, S. Marcinkevičius, A. Alkauskas, and C. G. van de Walle, Appl. Phys. Lett. **109**, 162107 (2016).
[25]D. Wickramaratne, J. X. Shen, C. E. Dreyer, A. Alkauskas, and C. G. van de Walle, Phys. Rev. B **99**, 205202 (2019).
[26]S. F. Chichibu, K. Shima, K. Kojima, S. Takashima, M. Edo, K. Ueno, S. Ishibashi, and A. Uedono, Appl. Phys. Lett. **112**, 211901 (2018).
[27]J. L. Lyons, A. Janotti, and C. G. Van de Walle, Phys. Rev. Lett. **108**, 156403 (2012).
[28]I. C. Diallo and D. O. Demchenko, Phys. Rev. Appl. **6**, 064002 (2016).
[29]J. L. Lyons and C. G. Van de Walle, npj Comput. Mater. **3**, 12 (2017).
[30]M. Horita, T. Narita, T. Kachi, and J. Suda, Appl. Phys. Lett. **118**, 012106 (2021).
[31]T. Kachi, T. Narita, H. Sakurai, M. Matys, K. Kataoka, K. Hirukawa, K. Sumida, M. Horita, N. Ikarashi, K. Sierakowski, M. Bockowski, and J. Suda, J. Appl. Phys. **132**, 130901 (2022).